Quantitative Changes in Perifoveal Capillary Networks in Patients With Vascular Comorbidities

Geoffrey Chan,[1,2] Chandrakumar Balaratnasingam,[1,2] Paula K. Yu,[1,2] William H. Morgan,[1] Ian L. McAllister,[1] Stephen J. Cringle,[1,2] and Dao-Yi Yu[1,2]

[1]Centre for Ophthalmology and Visual Science, The University of Western Australia, Perth, Australia
[2]The Australian Research Council Centre of Excellence in Vision Science, The University of Western Australia, Perth, Australia

Correspondence: Dao-Yi Yu, Centre for Ophthalmology and Visual Science, The University of Western Australia, 2 Verdun Street, Nedlands, Western Australia 6009; dyyu@cyllene.uwa.edu.au.

Submitted: February 28, 2013
Accepted: June 18, 2013

Citation: Chan G, Balaratnasingam C, Yu PK, et al. Quantitative changes in perifoveal capillary networks in patients with vascular comorbidities. *Invest Ophthalmol Vis Sci*. 2013;54:5175–5185. DOI:10.1167/iovs.13-11945

Purpose. To determine if patients with cardiovascular comorbidities but no clinically detectable retinal disease demonstrate quantitative alterations to perifoveal capillary networks.

Methods. Comparisons were made between 10 eyes from patients with vascular comorbidities and 17 control eyes. All eyes were absent of clinically evident ocular disease. Microcannulation techniques were used to label the retinal microvasculature. Retinae were flat mounted, and the peripapillary region 2 mm nasal to the fovea was imaged using confocal laser scanning microscopy. Two- and three-dimensional image reconstructions were used to perform quantitative measurements of individual capillary networks within the perifovea. Parameters measured included capillary diameter, capillary loop area, capillary loop length, capillary density, and capillary surface area.

Results. Capillary diameter was increased in the retinal ganglion cell and superficial inner plexiform layer capillary network in patients with vascular comorbidities. Capillary loop area and capillary loop length were reduced in all capillary networks in patients with vascular comorbidities except the deep capillary network of the inner nuclear layer. Capillary density was reduced in the nerve fiber layer capillary network in patients with vascular comorbidities. There was no difference in the relative occupied capillary surface area between control and diseased eyes.

Conclusions. The results in this study suggest that the quantitative characteristics of perifoveal capillary networks are nonuniformly altered in patients with vascular comorbidities, before the onset of clinically identifiable eye diseases. These findings may be important for understanding pathophysiological mechanisms involved in retinal vascular diseases.

Keywords: retina, capillary, fovea, vasculature, retinopathy, hypertension

The human retina is nourished by a layered network of capillaries that are morphometrically organized in accordance with the heterogeneic metabolic demands of neuronal subtypes.[1,2] Capillary endothelia facilitate the exchange of nutrients and toxic wastes between neurons and supporting glia.[3–5] By doing so they perform a critical role in modulating retinal homeostasis. Cardiovascular comorbidities have the potential to alter the blood–retina barrier (BRB) and are therefore considered important risk factors for retinal disease.[6,7] However, it is unknown if the quantitative characteristics of retinal capillary networks are altered before disease-induced alterations to the BRB become clinically manifest. Such knowledge is important as it may permit the application of emerging state-of-the-art technology to image capillary networks and thus detect early retinal disease.[3] Furthermore, because breakdown of the BRB results in vasogenic edema and neural tissue damage with resultant loss of vision,[4] the clinical application of such histopathologic knowledge could be of major benefit in the prevention of vision loss. Understanding capillary network changes in patients with cardiovascular comorbidities may provide valuable insights into pathogenic mechanisms that underlie retinal vascular diseases.

Utilizing novel microcannulation techniques developed in our laboratory, we have previously quantified the quantitative characteristics of capillary networks that serve the retina.[5–9] These studies have identified four different capillary networks in the normal human retina, the quantitative and morphometric characteristics of each network varying with retinal depth and eccentricity.[5,6] The present study employed two- and three-dimensional image analysis techniques to document perifoveal capillary network changes in patients with a history of cardiovascular morbidity but no clinically detectable retinal disease. We also determined if capillary networks are selectively or uniformly altered by cardiovascular morbidity. The purpose of this study was to investigate the consequence of cardiovascular morbidity on retinal capillary network morphometry. Results presented in the paper may allow clinico-histologic correlation with modern imaging devices to aid in the early detection of retinal vascular disease. As the retina is considered a window to the brain, findings in this report may also provide a valuable contribution to previous investigations that have demonstrated important relationships between retinal vascular characteristics and cardiovascular morbidity.[10–15]

Table 1. Donor Demographic Details: Sex, Age, Eye, Vascular Comorbidities, Cause of Death, and Time to Perfusion for Each Eye Donor

Patient ID	Sex	Age, y	Eye	Vascular Comorbidities	Cause of Death	Time to Perfusion, h
A	F	56	R+L	Hypercholesterolemia	Renal transplant failure	8.5
B	M	65	R+L	Hypertension, atherosclerosis	ICH	14
C	M	64	L	Hypertension	MI	14
D	M	60	R+L	Atrial fibrillation, hypertension, heart failure	MI	8.5
E	M	64	L	Hypertension, dyslipidemia	MI	22
F	M	79	R+L	Hypertension, atherosclerosis	ICH	15
G	M	32	L	-	MVA	20
H	M	23	L	-	Suicide	22
I	M	53	L	-	MVA	14
J	M	66	R+L	-	Metastatic colon cancer	15
K	M	22	L	-	Suicide	15
L	M	27	L	-	MVA	8
M	M	59	R+L	-	Melanoma	12
N	M	39	R+L	-	Bacterial endocarditis	20
O	M	15	R+L	-	Hanging	22.5
P	M	19	R	-	Hanging	17
Q	M	67	L	-	Metastatic lung cancer	12
R	F	73	R	-	Metastatic breast cancer	15

R, right; L, left; ICH, intracranial hemorrhage; MI, myocardial infarction; MVA, motor vehicle accident. Line separates disease and control eyes.

Materials and Methods

This study was approved by the human research ethics committee at The University of Western Australia. All human tissue was handled according to the tenets of the Declaration of Helsinki.

Human Donor Eyes

Human donor eyes used for this research were absent of clinically evident ocular disease. Ocular disease in donor eyes was excluded using patient records, postmortem examination by an ophthalmologist, and also examination of retinal flat mounts with a fluorescent microscope after perfusion. Specifically, examination of retinal flat mounts did not demonstrate the presence of microaneurysms, neovascular vessels, leakage, arterial/vein occlusions, vascular anomalies, or areas of retina nonperfusion in donor eyes. A total of 10 human eyes from 6 donors with vascular comorbidities and 17 control eyes from 12 donors were used. Most of the control eyes used in this study were also used in our previous work.[6] Additionally, 6 control eyes from 4 new donors were used; 2 of these donors died from hanging (ages 15 and 19 years), and the other 2 died from metastatic cancer (ages 67 and 73 years). In this study, the group with cardiovascular comorbidities is referred to as the disease group, and control donors are referred to as the control group. Patients in the disease group suffered from one or more of the following vascular comorbid conditions: hypertension, congestive cardiac failure, dyslipidemia, atherosclerosis, atrial fibrillation, or hypercholesterolemia (Table 1). All eyes were obtained from the Lions Eye Bank of Western Australia (Lions Eye Institute, Western Australia). The demographic data and vascular comorbidities of each donor are presented in Table 1.

Tissue Preparation

Our previously reported method of microcannulation and targeted perfusion-based labeling techniques was utilized to label the retinal microvasculature.[5–9] The central retinal artery was cannulated using a glass micropipette, and the retinal circulation was perfused for 20 minutes with a mixture of oxygenated Ringer's solution and 1% bovine serum albumin. A solution of 4% paraformaldehyde in 0.1 M phosphate buffer was then used for perfusion-fixation with permeabilization of endothelial cell membranes aided by a 0.1% Triton X-100 in 0.1 M phosphate buffer solution. Detergent was removed from the retinal circulation by perfusion with 0.1 M phosphate buffer solution. Endothelial microfilaments were labeled over 2 hours by perfusion with a solution comprising either phalloidin conjugated to Alexa Fluor 546 (30 U, A22283; Invitrogen, Carlsbad, CA) or lectin-TRITC[16] (1:40, L5266; Sigma-Aldrich, St. Louis, MO). Nucleus labeling was achieved with bisbenzimide (1.2 μg/mL; Sigma-Aldrich). Residual label was cleared from the vasculature by further perfusion with 0.1 M phosphate buffer. Labeled specimens were immersion fixed in 4% paraformaldehyde overnight prior to dissection and flat mounting.

Microscopy

The perifoveal region, located 2 mm nasal to the center of the fovea, was imaged using confocal laser scanning microscopy.[17] The region that was studied occupied an area of 4.1×10^5 μm^2. The perifovea was examined because we had previously quantified the morphometric characteristics of capillary networks in this region in normal human eyes and thus were able to make direct and reliable comparisons with eyes from patients with cardiovascular comorbidities.[6] The other reason the perifovea was analyzed was that it is traversed by the macula–papillary bundle and thus plays a critical role in visual processing. Furthermore, unlike the peripheral retina, which is composed of only a single row of ganglion cells, the nasal perifovea is characterized by four or five rows of retinal ganglion cells.[17] Wide-field images utilizing a ×4 dry lens (Plan numerical aperture [NA] 0.2; Nikon, Tokyo, Japan) and a fluorescent microscope (Eclipse E800; Nikon) were used to accurately measure distances from the center of the fovea prior to confocal scanning. Confocal microscope images were captured using a Nikon C1 Confocal with EZ-C1 (version 3.20) image acquisition software. A ×20 dry objective lens (NA 0.4) was used for all scans. Using a motorized stage, a series of z-stacks were captured for each specimen beginning from the vitreal surface at the level of the inner limiting membrane to the outer retina. Each z-stack consisted of a depth of optical

sections collected at 0.35-μm increments along the z-plane. Visualization of sections was achieved by sequential laser excitation at a 488- and 561-nm line from an argon laser with emissions detected through a 525/50-nm 595/40-nm band pass filter, respectively.

Image Preparation

ImagePro Plus (version 7.1; Media Cybernetics, Rockville, MD) and ImageJ (version 1.43; http:/rsb.info.nih.gov/ij [provided in the public domain by National Institutes of Health, Bethesda, MD]) software were used to quantify confocal microscope images. All images for the manuscript were prepared using Adobe Photoshop (version 12.1; Adobe Systems, Inc., San Jose, CA) and Adobe Illustrator CS5 (version 12.1.0; Adobe Systems, Inc.). Confocal images in this manuscript were pseudo-colored using Look Up Tables available on ImageJ.

Three-dimensional reconstruction of capillary networks was performed using Imaris software (version 7.4.2; Bitplane, Zurich, Switzerland). To minimize artifact caused by minor fluctuations in signal intensity, the dataset was refined by utilizing the Gaussian filter tool and background subtraction prior to three-dimensional reconstruction.[6]

Qualitative Differentiation of Capillary Networks

Our previously defined morphometric criteria, which have been validated by interobserver correlation studies, were used to partition the retinal circulation into separate capillary networks.[5,6] Capillary branching patterns, trajectory, and position respective to nuclear layers were used to stratify the retinal circulation into separate networks. Qualitative studies were performed only on eyes from the disease group, as we had previously reported the characteristics of different networks in normal eyes.[6]

Morphometric Quantification of Capillary Networks

Our previously published methods were used to quantify the morphometric features of capillary networks in the disease group.[6] Manual tracing methods using ImageJ software (version 1.43; National Institutes of Health) were employed to obtain capillary diameter, capillary loop area, capillary loop length, and capillary density measurements from each network.[18–22] Capillary loop area was defined as the area enclosed by regional capillaries that intersected to form a closed loop within a network. The boundary of individual capillary loops in each network was determined by carefully scrolling through image slices within the stack. Three-dimensional image reconstructions (described below) were also used to accurately delineate the boundaries of capillary loops. Once the boundaries of individual capillary loops were determined, the z-projected image of the stack was used to calculate the loop area. Capillary loop length was calculated by measuring the maximal linear distance between capillary loop apices formed by z-projected capillary loops.

Capillary density was determined by calculating the percentage of the image that was occupied by capillary lumens. Manual tracing techniques were used to determine the area of the image occupied by capillary lumens. Capillary density was determined by dividing this measurement by the total area of the image. In some eyes, data could not be obtained from all capillary networks due to limitations in image quality.

Imaris (Bitplane) statistics sum function was applied to three-dimensional image reconstructions to express the surface area of each capillary network as a proportion of the total surface area occupied by capillaries in the perifoveal region. This calculation was performed using eyes in the control and disease groups and is referred to as the relative occupied capillary surface area.

Statistical Analysis

All data are expressed in terms of mean and standard error, which were calculated using R (R Foundation for Statistical Computing, Vienna, Austria). The disease eye cohort data were initially analyzed followed by comparisons with control groups. In the disease group analysis, capillary network layer and postmortem time were assigned as covariates and morphometric measurements as the response variable. Multiple measurements from eyes, with data taken from right and left eyes of the same individual, were analyzed with right or left eye nested within eye donor, assigned as random effects to account for factor correlations.[23] Analysis of covariance (ANCOVA) testing between four capillary networks generated three comparisons; thus a P value of <0.017 was considered significant.

In the analysis comparing disease and control eye cohorts, we grouped measurements from a single capillary network. Similarly, group (control or disease group) and postmortem time were assigned as covariates with morphometric measurements as the response variable. Right or left eyes nested within eye donor were assigned as random effects to account for factor correlations.[23] For these comparisons, ANCOVA testing was performed with a P value of <0.050 considered significant.

Results

Eye Donors

The mean age of donors in the control group was 43.6 ± 5.1 years (range, 15–73 years). We examined 5 right eyes and 12 left eyes from a total of 12 donors (10 male, 2 female). The average postmortem time before eyes were perfused was 15.7 ± 1.3 hours.

The mean age of donors in the disease group was 64.8 ± 2.5 (range, 56–79 years). We examined 4 right eyes and 6 left eyes from a total of 6 donors (5 male, 1 female). The average postmortem time before eyes were perfused was 12.2 ± 1.4 hours. There was a significant difference between the mean age of donor eyes in the disease and control groups ($P = 0.005$).

General

All orders of retinal microvasculature were clearly identifiable by our perfusion labeling technique. The position and morphology of separate capillary networks in disease eyes were similar to what we observed in control eyes.[5,6] We identified four separate capillary networks in disease eyes corresponding to the following regions within the retina: the nerve fiber layer (NFL), the retinal ganglion cell/superficial inner plexiform layer (RGC/sIPL), the deep inner plexiform layer/superficial inner nuclear layer (dIPL/sINL), and the deep inner nuclear layer (dINL).

A total of 1348 capillary diameter and 315 capillary loop area measurements were made in control eyes. A total of 1547 capillary diameter and 280 capillary loop area measurements were performed in disease eyes.

Investigative Ophthalmology & Visual Science

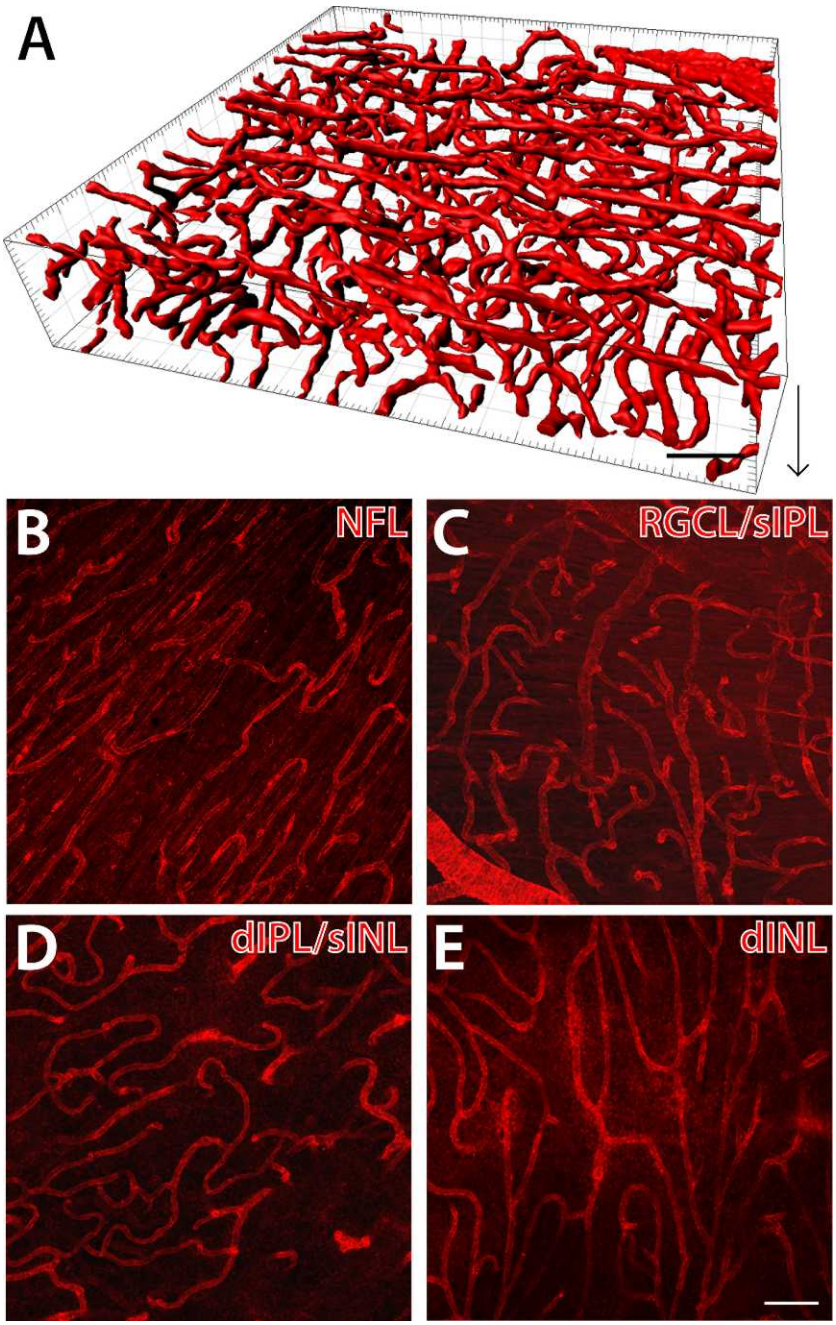

FIGURE 1. Three-dimensional reconstruction of human perifoveal capillary networks in an eye with vascular comorbidities (**A**). Confocal capillary images captured from a single laser channel demonstrate the NFL network (**B**), RGC/sIPL network (**C**), dIPL/sINL network (**D**), and dINL network (**E**). *Arrow* indicates direction from vitread to sclerad surface. *Scale bar*: 100 μm.

Morphometric Characteristics of Capillary Networks in Disease Eyes

Morphometric characteristics of the four different capillary networks in diseased eyes are shown in Figure 1.

NFL Capillary Network. Capillaries of the NFL network were characterized by a predominance of capillary segments that were oriented parallel to the direction of retinal ganglion cell axons (Fig. 1B). Short interconnecting segments bridged these capillaries in a diagonal or perpendicular fashion. Mean capillary diameter in the NFL network was 8.64 ± 0.06 μm. Mean capillary loop area was 2496.36 ± 713.48 μm^2. Mean capillary loop length in the NFL network was 83.25 ± 17.14 μm. Capillary density in the NFL network was 12.78% ± 1.66%. Mean relative occupied capillary surface area was 13.62% ± 2.31%. NFL capillary measurements from individual donors are presented in Table 2.

RGC/sIPL Capillary Network. Capillaries of the RGC/sIPL network were characterized by a dense meshwork of three-dimensional vessels (Fig. 1C). Reduced intercapillary distance was a predominant feature of this network with capillary segments demonstrating sharp diagonal and orthogonal branching patterns. Mean capillary diameter in the RGC/sIPL network was 8.93 ± 0.07 μm. Mean capillary loop area was 1734.01 ± 141.66 μm^2. Mean capillary loop length in the RGC/sIPL network was 62.41 ± 3.10 μm. Capillary density in

Investigative Ophthalmology & Visual Science

TABLE 2. Quantitative Capillary Network Data for Individual Donors: Mean Capillary Diameter, Capillary Loop Area, Capillary Density, and Relative Capillary Surface Area Measurements for Each Donor Eye

	Capillary Diameter, μm				Capillary Loop Area, μm²				Capillary Density, %				Relative Capillary Surface Area, %			
Specimen	NFL	RGCL/sIPL	dIPL/sINL	dINL	NFL	RGCL/sIPL	dIPL/sINL	dINL	NFL	RGCL/sIPL	dIPL/sINL	dINL	NFL	RGCL/sIPL	dIPL/sINL	dINL
A	8.9	9.0	9.0	-	10164.8	1473.4	5453.3	-	17.7	29.5	22.8	-	-	-	-	-
A	8.7	9.1	9.6	-	0.0	2513.5	4244.1	-	14.0	27.4	25.4	-	-	-	-	-
B	8.6	9.0	8.2	8.6	1802.0	1308.7	3878.1	6287.1	21.2	23.1	14.8	20.4	22.8	30.5	21.5	25.1
B	9.6	8.7	9.2	8.5	3041.8	1084.0	3794.5	5661.9	14.1	34.3	18.9	18.6	13.9	47.8	15.4	22.8
C	6.8	8.1	8.8	-	2434.9	1551.8	3186.9	-	4.3	18.3	13.8	-	-	-	-	-
D	8.6	9.4	9.4	9.7	623.9	1834.1	3420.0	5123.7	15.4	27.6	17.2	29.4	17.3	31.7	20.6	30.4
D	9.1	8.9	9.0	9.9	0.0	1521.1	824.4	5793.9	14.6	28.2	18.1	29.8	10.5	55.8	13.4	20.3
E	9.2	9.3	-	-	0.0	5429.6	-	-	12.6	14.9	-	-	-	-	-	-
F	8.3	8.6	8.6	8.8	3180.5	1967.6	0.0	11025.0	7.2	26.3	9.9	17.8	7.8	46.5	13.8	31.9
F	9.1	8.8	8.8	9.0	1732.6	2606.0	1416.1	4038.5	6.7	24.8	18.9	21.2	9.4	30.9	31.4	28.2

Hyphen designates data that could not be obtained.

the RGC/sIPL network was 25.46% ± 1.76%. Mean relative occupied capillary surface area was 40.55% ± 4.44%. RGC/sIPL capillary measurements from individual donors are presented in Table 2.

dIPL/sINL Capillary Network. Capillaries in the dIPL/sINL network were highly tortuous and demonstrated irregular-shaped loop configurations (Fig. 1D). Mean capillary diameter in the dIPL/sINL network was 8.96 ± 0.06 μm. Mean capillary loop area was 2813.66 ± 427.61 μm². Mean capillary loop length in the dIPL/sINL network was 73.86 ± 6.49 μm. Capillary density in the dIPL/sINL network was 17.77% ± 1.55%. Mean relative occupied capillary surface area was 19.35% ± 2.79%. dIPL/sINL capillary measurements from individual donors are presented in Table 2.

dINL Capillary Network. Capillaries of the dINL network were characterized by a predominantly one-dimensional laminar configuration where capillaries ran a trajectory with little tortuosity (Fig. 1E). Mean capillary diameter in the dINL network was 9.10 ± 0.07 μm. Mean capillary loop area was 6004.32 ± 526.20 μm². Mean capillary loop length in the dINL network was 147.86 ± 9.46 μm. Capillary density in the dINL network was 21.55% ± 1.38%. Mean relative occupied capillary surface area was 26.48% ± 1.83%. dINL capillary measurements from individual donors are presented in Table 2.

Comparisons Between Capillary Networks in Disease Eyes

Age was not associated with capillary diameter, loop area, loop length, density, or occupied capillary surface area measurements in any of the control ($P > 0.107$) or disease networks ($P > 0.172$). Capillary diameter was smallest in the NFL network and was significantly smaller than in the RGC/sIPL network ($P = 0.001$) and dIPL/sINL network ($P = 0.002$), but not the dINL network ($P = 0.062$). There was no difference in capillary diameter between the RGC/sIPL network and dIPL/sINL network ($P = 0.489$). There was also no difference in capillary diameter between RGC/sIPL and dINL networks ($P = 0.205$).

Capillary loop area was smallest in the RGC/sIPL network and was significantly smaller than in the dIPL/sINL and dINL networks (all $P < 0.003$), but not the NFL network ($P = 0.086$). Capillary loop area was largest in the dINL network and was significantly larger than in the NFL, RGC/sIPL, and dIPL/sINL networks (all $P < 0.003$). Capillary loop area was not significantly different between the NFL and dIPL/sINL networks ($P = 0.738$).

Capillary loop length was largest in the dINL network and was significantly larger than in the NFL, RGC/sIPL, and dIPL/sINL networks (all $P < 0.003$). Capillary loop length was smallest in the RGC/sIPL network and was significantly smaller than in the dINL ($P < 0.001$), but not the NFL ($P = 0.062$) or dIPL/sINL network ($P = 0.035$). Capillary loop length was not significantly different between the NFL and dIPL/sINL networks ($P = 0.292$).

Capillary density was smallest in the NFL network and was significantly smaller than in the RGC/sIPL network ($P = 0.001$) and dINL network ($P = 0.011$), but not the dIPL/sINL network ($P = 0.043$). Capillary density was significantly smaller in the dIPL/sINL network than in the RGC/sIPL network ($P = 0.001$). There was no difference in capillary density between the dINL network and the RGC/sIPL network ($P = 0.075$) and dIPL/sINL network ($P = 0.017$).

Relative occupied capillary surface area was greatest in the RGC/sIPL network and was significantly greater than in the NFL ($P = 0.004$) and dIPL/sINL ($P = 0.012$) networks, but not in the dINL network ($P = 0.038$). Relative occupied capillary surface area was significantly larger in the dINL than in the

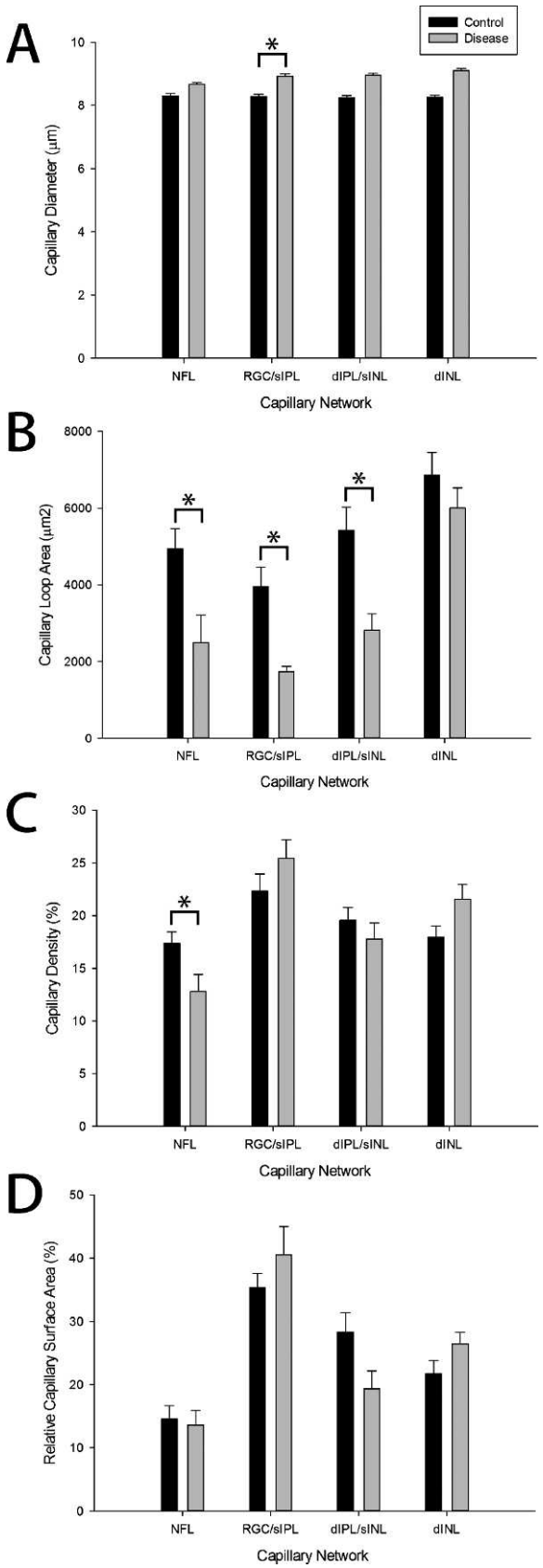

FIGURE 2. Quantitative comparisons of capillary network morphometry. Comparisons between control and disease eyes for capillary diameter (**A**), capillary loop area (**B**), capillary density (**C**), and relative occupied capillary surface area (**D**) are presented. Mean ± standard error for each parameter is provided. *Asterisk* denotes a significant difference between control and disease eyes ($P < 0.05$).

NFL ($P = 0.010$). There was no difference in capillary surface area between the dIPL/sINL and the NFL ($P = 0.152$) or the dINL network ($P = 0.055$).

Comparisons Between Disease and Control Eyes

Morphometric comparisons between control and disease eyes are displayed as bar charts in Figure 2. Morphometric comparisons between control and disease eyes for NFL, RGC/sIPL, dIPL/sINL, and dINL networks are provided in Figure 3. Comparisons of the three-dimensional characteristics of these networks are provided in Figure 4.

NFL Capillary Network. There was no difference in NFL capillary diameter between disease and control groups ($P = 0.469$). Capillary loop area ($P = 0.020$), capillary loop length ($P = 0.009$), and density ($P = 0.033$) were reduced in disease eyes (Figs. 3A, 3B, 4A). There was no difference in relative occupied capillary surface area between disease and control groups ($P = 0.279$).

RGC/sIPL Capillary Network. Capillary diameter in the RGC/sIPL network in the disease group was greater than in control eyes ($P = 0.005$). Disease eyes had smaller capillary loop area ($P = 0.001$) and capillary loop lengths ($P = 0.003$); however, there was no significant difference in capillary density ($P = 0.271$) between the two groups (Figs. 3C, 3D, 4B). There was no difference in relative occupied capillary surface area between disease and control groups ($P = 0.218$).

dIPL/sINL Capillary Network. There was no difference in dIPL/sINL capillary diameter between disease and control groups ($P = 0.065$). Disease eyes had smaller capillary loop areas ($P = 0.008$) and capillary loop lengths ($P = 0.005$), but there was no significant difference in capillary density ($P = 0.173$) between the two groups (Figs. 3E, 3F, 4C). There was no difference in relative occupied capillary surface area between disease and control groups ($P = 0.061$).

dINL Capillary Network. There was no difference in dINL capillary diameter between disease and control groups ($P = 0.073$). There was no difference in capillary loop area ($P = 0.863$), capillary loop length ($P = 0.444$), capillary density ($P = 0.075$), and relative occupied capillary surface area ($P = 0.440$) between the two groups (Figs. 3G, 3H, 4D).

DISCUSSION

The major findings from this study are as follows. First, cardiovascular comorbidities induce alterations to capillary diameter, capillary loop area, and capillary density measurements within the human perifovea. Second, capillary networks are altered in a nonuniform manner by cardiovascular comorbidities. Specifically, capillary diameter increased in the RGC/sIPL network. Capillary loop length and capillary loop area decreased in all networks other than the deep INL network in patients with cardiovascular comorbidities. Capillary density was reduced in the NFL network only.

Capillary endothelia maintain intimate relationships with neurons and glia cells and thereby modulate retinal homeostasis.[24–28] The morphometric organization and position of capillary networks, within the layered retina, are believed to correlate with the metabolic demands of regional neuronal subtypes.[1,2,27–32] Quantifiable parameters such as capillary loop area, capillary loop length, capillary density, and capillary diameter convey vital information about the vasculogenic mechanisms that are involved in retinal nutrition.[19–22] Through the complex process of neurovascular coupling, capillary diameter is linked to mean erythrocyte transit time through a microcirculation and contributes to the tissue oxygen extraction fraction.[29,30] Similarly, capillary loop area and density

Investigative Ophthalmology & Visual Science

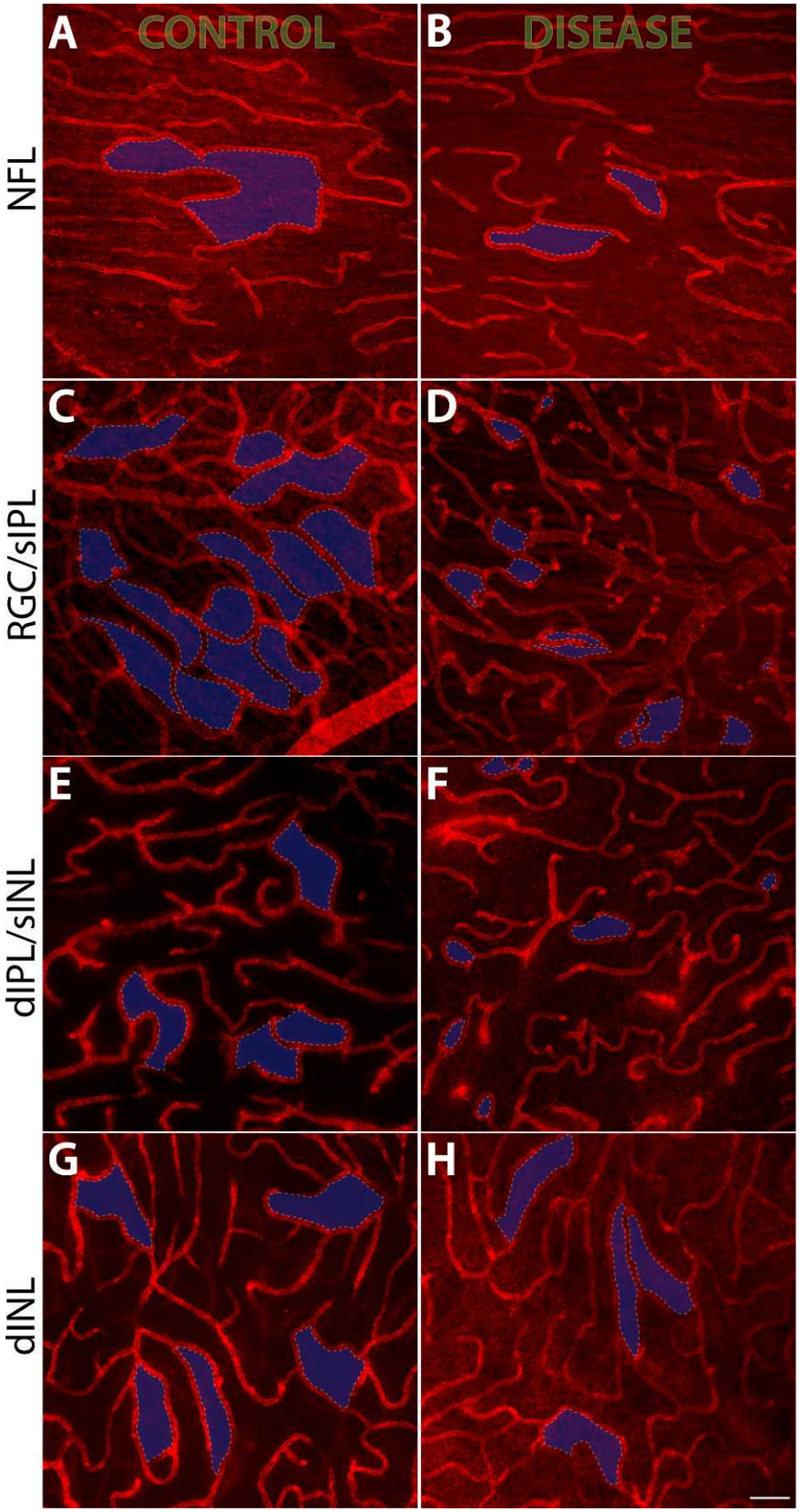

FIGURE 3. Morphometric comparisons between control and disease eyes for NFL (**A**, **B**), RGC/sIPL (**C**, **D**), dIPL/sINL (**E**, **F**), and dINL (**G**, **H**) networks. Some capillary loops in each image are shaded in *blue* to allow comparison of capillary loop area between the two groups. *Scale bar*: 100 μm.

Investigative Ophthalmology & Visual Science

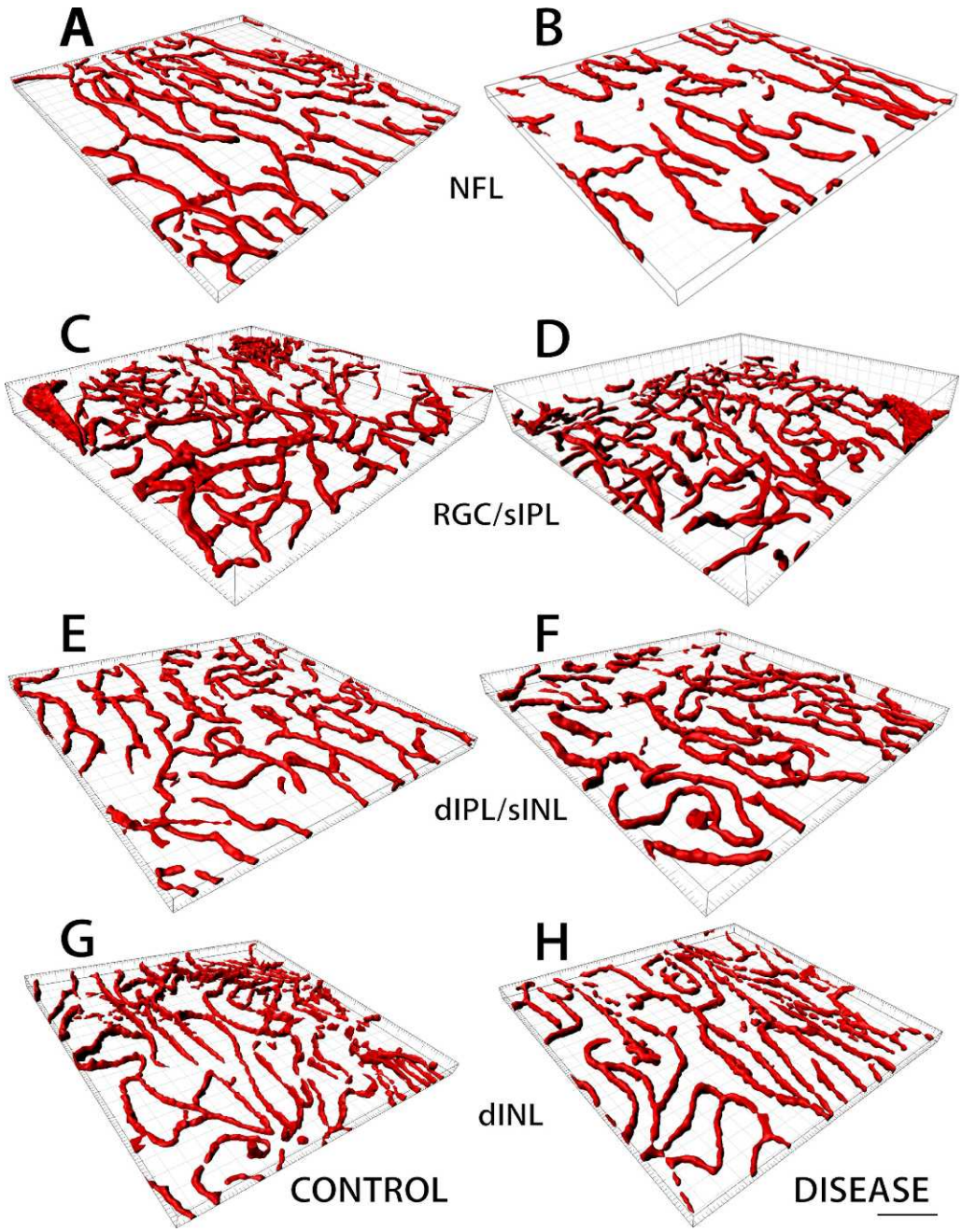

FIGURE 4. Comparison of three-dimensional capillary network morphometry between control and disease eyes. There was no difference in relative occupied surface area between the two groups in the NFL network (**A**, **B**), RGC/sIPL network (**C**, **D**), dIPL/sINL network (**E**, **F**), and dINL network (**G**, **H**). *Scale bar*: 200 μm.

measurements allow inference about diffusion mechanisms that are involved in satisfying regional energy demands.[22,31–34]

Cardiovascular comorbidities, including ischemic heart disease, hypertension, smoking, and hypercholesterolemia, have been implicated in the pathogenesis of retinal vascular disease.[10,12,14,15,35–39] Detailed histopathologic studies have demonstrated alterations to endothelial tight junctions, basement membranes, and mural cells in patients with cardiovascular disease.[12,13,35] The net effect of these histologic changes is the breakdown of the BRB. Clinical manifestations of BRB perturbations include microaneurysms, exudates, hemorrhages, edema, and nerve fiber layer ischemia.[15,22,40–42] When present in the macula or perifovea, these changes can result in rapid and irreversible vision loss.[43] Although transverse histologic investigations have been used to study circulatory changes in the eye,[44–46] to our knowledge, two- and three-dimensional quantitative techniques have not been employed to quantify disease-induced capillary network alteration in the human retina. The chronological relationship between retinal capillary network alteration and endothelial dysfunction, whether it is antecedent or subsequent, has also not been explored. This information may be important for understanding pathophysiological mechanisms involved in retinal vascular diseases.

In this study, capillary loop area measurements were used to speculate upon the role of diffusion mechanisms in regional cellular nutrition. Mathematical studies have shown that steady-state oxygen diffusion in vascular networks with an arbitrary geometry can be modeled to a three-dimensional space.[47–49] Therefore, although the two- and three-dimensional configuration of capillary loops was different between networks, it is likely that the functional properties of each loop with regard to oxygen diffusion are similar. The present study demonstrated a decrease in capillary loop area in all retinal networks, other than the dINL, in patients with cardiovascular comorbidities. Decreasing intercapillary areas may result in decreased oxygen diffusion times and may therefore be an important compensatory mechanism by which the microcirculation ensures adequate cellular nutrition in early retinal disease.[22,34] The proximity of the deep inner nuclear layer to the outer retina, where the choroid is the predominant supplier of metabolic substrates,[46] may have been the reason why capillary loop areas were not altered in this network.

In the capillary network subserving the retinal ganglion cell and superficial inner plexiform layer, the mean diameter of capillaries in patients with cardiovascular comorbidities is increased. These findings are similar to what has been described in cerebrocortical models of hypoxia.[48] In the parietal cortex, experimental hypoxia induces heterogeneous changes to capillary network flow and also an increase in red blood cell velocity.[50] Disease-induced increases in capillary diameter are speculated to underlie these changes.[51] Capillary diameter in the brain has also been shown to increase in hypercapnic hyperemia.[51–53] The net effect of increasing capillary diameter is an increase in blood flow and thus improved tissue oxygenation.[54] Such an increase in capillary diameter may explain, at least to some degree, the "non-difference" in corresponding capillary density and occupied surface area measurements between disease and control eyes. Patients with cardiovascular comorbidities may experience some degree of retinal hypoxia relative to normal eyes. We speculate that in the earliest stages of hypertension and other cardiovascular comorbid disorders, a compensatory increase in capillary diameter may be one means of satisfying neuronal demands in a relatively hypoxic environment before later clinical disease such as decreased arteriolar diameter becomes manifest.[15]

The molecular basis for capillary network alteration in patients with cardiovascular comorbidities may be the upregulation of cytokines and growth factor gradients within the retina.[13,55,56] Vascular endothelial growth factor (VEGF) is a major stimulator of endothelial movement and an important determinant of capillary network morphology in embryogenesis.[57,58] Other growth factors involved in vasculogenesis include fibroblast growth factor and transforming growth factor beta.[59,60] We speculate that upregulation of growth factors in the retina in patients with cardiovascular comorbidities, possibly due to hypoxia, may underlie the process of capillary network alteration. Disease-induced VEGF expression in the retina is nonuniform, being predominantly expressed by Müller cells, endothelia, astrocytes, retinal pigment epithelium, and retinal ganglion cells.[61] The nonuniform pattern of capillary network alteration in patients with cardiovascular comorbidities may bear important correlations to the predominant cell type that is activated to produce VEGF in the presence of cardiovascular disease. Further work, however, is required to explore these correlations.

Microcannulation techniques employed in this study allowed complete labeling of the retinal circulation and permitted us to reliably quantify the morphometric features of capillary networks in the perifovea. The results of this study suggest that capillary network morphometry is altered before clinical signs of BRB breakdown are evident in patients with cardiovascular comorbidities. Our previous study compared the morphometric features of human retinal capillary networks between images derived from fluorescein angiography and postmortem histopathologic slides.[44] That study showed that capillary details derived from fluorescein angiography and fundus photography are limited to the inner capillary networks, with very little information concerning the deep networks present in images derived by these modalities. The density of capillary structures in fluorescein images is also significantly lower than in images derived from the same retinal eccentricity by confocal scanning laser microscopy techniques using postmortem tissue. Therefore, current imaging modalities that are employed in clinical practice do not allow a layered analysis of human capillary networks.[44] However, the emergence of high-penetration optical coherence tomography technology[3] may permit noninvasive means of studying distinct capillary networks in the human eye and may be useful for the early detection of capillary alteration in patients with cardiovascular comorbidities. Application of such technologies to monitor the temporal sequence of capillary network alteration in at-risk patients may also allow the timely intervention of therapy.

Although this report provides valuable information concerning the pathogenesis of retinal vascular disease, we acknowledge several limitations of the study. The sample size in this study was too small to separate the effects of individual vascular comorbid disease on capillary network morphometry. The spectrum of systemic disease severity for each donor was also unknown. Furthermore, if the sample size had been larger, it would have been useful to compare the morphometric features of capillary networks between treated and untreated patients in the disease group.

It is also possible that some of the control donors were suffering from undiagnosed vascular comorbidities at the time of death, and this remains a limitation with all postmortem histopathologic studies. The findings of this study are also limited to one retinal eccentricity. It is possible that capillary network alteration is specific to the form of cardiovascular insult and retinal eccentricity. The purpose of this study was to investigate the effects of cardiovascular risk factors on the retinal microcirculation; and although there was no documented evidence of cardiovascular comorbidity in the control group, some of the patients in this group may not have been healthy at the time of death. This in turn may have had some influence on the results of this study. Other limitations of this study include the potential of postmortem alterations to vascular morphology and the long postmortem time, greater than 12 hours, in four patients in the disease group.

Acknowledgments

The authors thank staff from the Lions Eye Bank of Western Australia, Lions Eye Institute, for provision of human donor eyes and staff from DonateWest, the Western Australian agency for organ and tissue donation, who facilitated the recruitment of donors into the study by referral and completion of consent processes. We also thank Dean Darcey for his expert technical assistance.

Supported by grants from the National Health and Medical Research Council of Australia and the Australian Research Council Centre of Excellence in Vision Science.

Disclosure: **G. Chan**, None; **C. Balaratnasingam**, None; **P.K. Yu**, None; **W.H. Morgan**, None; **I.L. McAllister**, None; **S.J. Cringle**, None; **D.-Y. Yu**, None

References

1. Yu D-Y, Cringle SJ. Oxygen distribution and consumption within the retina in vascularised and avascular retinas and in animal models of retinal disease. *Prog Retina Eye Res*. 2001; 20:175–208.
2. Pournaras CJ, Rungger-Brandle E, Riva CE, Hardarson SH, Stefansson E. Regulation of retinal blood flow in health and disease. *Prog Retin Eye Res*. 2008;27:284–330.
3. Makita S, Jaillon F, Yamanari M, Miura M, Yasuno Y. Comprehensive in vivo micro-vascular imaging of the human eye by dual-beam-scan Doppler optical coherence angiography. *Opt Express*. 2011;19:1271–1283.
4. Klaassen I, Van Noorden CJ, Schlingemann RO. Molecular basis of the inner blood-retinal barrier and its breakdown in diabetic macular edema and other pathological conditions. *Prog Retin Eye Res*. 2013;34:19–48.
5. Tan PE, Yu PK, Balaratnasingam C, et al. Quantitative confocal imaging of the retinal microvasculature in the human retina. *Invest Ophthalmol Vis Sci*. 2012;53:5728–5736.
6. Chan G, Balaratnasingam C, Yu PK, et al. Quantitative morphometry of perifoveal capillary networks in the human retina. *Invest Ophthalmol Vis Sci*. 2012;53:5502–5514.
7. Yu PK, Balaratnasingam C, Cringle SJ, McAllister IL, Provis J, Yu DY. Microstructure and network organization of the microvasculature in the human macula. *Invest Ophthalmol Vis Sci*. 2010;51:6735–6743.
8. Yu PK, Tan PE, Morgan WH, Cringle SJ, McAllister IL, Yu DY. Age-related changes in venous endothelial phenotype at human retinal artery-vein crossing points. *Invest Ophthalmol Vis Sci*. 2012;53:1108–1116.
9. Kang MH, Balaratnasingam C, Yu P, et al. Morphometric characteristics of central retinal artery and vein endothelium in the normal human optic nerve head. *Invest Ophthalmol Vis Sci*. 2011;52:1359–1367.
10. London A, Benhar I, Schwartz M. The retina as a window to the brain-from eye research to CNS disorders. *Nat Rev Neurol*. 2013;9:44–53.
11. Cooper ME, Bonnet F, Oldfield M, Jandeleit-Dahm K. Mechanisms of diabetic vasculopathy: an overview. *Am J Hypertens*. 2001;14:475–486.
12. Wong TY, Hubbard LD, Klein R, et al. Retinal microvascular abnormalities and blood pressure in older people: the Cardiovascular Health Study. *Br J Ophthalmol*. 2002;86: 1007–1013.
13. Durham JT, Herman IM. Microvascular modifications in diabetic retinopathy. *Curr Diab Rep*. 2011;11:253–264.
14. Kawasaki R, Xie J, Cheung N, et al. Retinal microvascular signs and risk of stroke: the Multi-Ethnic Study of Atherosclerosis (MESA). *Stroke*. 2012;43:3245–3251.
15. Cheung CY, Ikram MK, Sabanayagam C, Wong TY. Retinal microvasculature as a model to study the manifestations of hypertension. *Hypertension*. 2012;60:1094–1103.
16. Gariano RF, Iruela-Arispe ML, Sage EH, Hendrickson AE. Immunohistochemical characterization of developing and mature primate retinal blood vessels. *Invest Ophthalmol Vis Sci*. 1996;37:93–103.
17. Hogan MJ, Alvarado JA, Esperson Weddell J. *Histology of the Human Eye: An Atlas and Textbook*. Philadelphia: W.B. Saunders; 1971.
18. Richard E, van Gool WA, Hoozemans JJ, et al. Morphometric changes in the cortical microvascular network in Alzheimer's disease. *J Alzheimers Dis*. 2010;22:811–818.
19. Sposito NM, Gross PM. Morphometry of individual capillary beds in the hypothalamo-neurohypophysial system of rats. *Brain Res*. 1987;403:375–379.
20. Shaver SW, Sposito NM, Gross PM. Quantitative fine structure of capillaries in subregions of the rat subfornical organ. *J Comp Neurol*. 1990;294:145–152.
21. Shaver SW, Pang JJ, Wall KM, Sposito NM, Gross PM. Subregional topography of capillaries in the dorsal vagal complex of rats: I. Morphometric properties. *J Comp Neurol*. 1991;306:73–82.
22. Arend O, Wolf S, Remky A, et al. Perifoveal microcirculation with non-insulin-dependent diabetes mellitus. *Graefes Arch Clin Exp Ophthalmol*. 1994;232:225–231.
23. R Development Core Team. *R: A Language and Environment for Statistical Computing*. Vienna, Austria: R Foundation for Statistical Computing; 2011.
24. Yu PK, Balaratnasingam C, Morgan WH, Cringle SJ, McAllister IL, Yu DY. The structural relationship between the microvasculature, neurons, and glia in the human retina. *Invest Ophthalmol Vis Sci*. 2010;51:447–458.
25. Metea MR, Newman EA. Glial cells dilate and constrict blood vessels: a mechanism of neurovascular coupling. *J Neurosci*. 2006;26:2862–2870.
26. Attwell D, Buchan AM, Charpak S, Lauritzen M, Macvicar BA, Newman EA. Glial and neuronal control of brain blood flow. *Nature*. 2010;468:232–243.
27. Drake CT, Iadecola C. The role of neuronal signaling in controlling cerebral blood flow. *Brain Lang*. 2007;102:141–152.
28. Yu DY, Cringle SJ, Yu PK, Su EN. Intraretinal oxygen distribution and consumption during retinal artery occlusion and graded hyperoxic ventilation in the rat. *Invest Ophthalmol Vis Sci*. 2007;48:2290–2296.
29. Jespersen SN, Ostergaard L. The roles of cerebral blood flow, capillary transit time heterogeneity, and oxygen tension in brain oxygenation and metabolism. *J Cereb Blood Flow Metab*. 2012;32:264–277.
30. Bedggood P, Metha A. Direct visualization and characterization of erythrocyte flow in human retinal capillaries. *Biomed Opt Express*. 2012;3:3264–3277.
31. Rackl A, Pawlik G, Bing RJ. Cerebral capillary topography and red cell flow in vivo. In: Ceros-Navaroo J, Fritschka E, eds. *Cerebral Microcirculation and Metabolism*. New York: Raven Press; 1981:17–21.
32. Pawlik G, Rackl A, Bing RJ. Quantitative capillary topography and blood flow in the cerebral cortex of cats: an in vivo microscopic study. *Brain Res*. 1981;208:35–58.
33. Remky A, Wolf S, Knabben H, Arend O, Reim M. Perifoveal capillary network in patients with acute central retinal vein occlusion. *Ophthalmology*. 1997;104:33–37.
34. Arend O, Wolf S, Jung F, et al. Retinal microcirculation in patients with diabetes mellitus: dynamic and morphological analysis of perifoveal capillary network. *Br J Ophthalmol*. 1991;75:514–518.
35. Wong TY, Klein R, Klein BE, Tielsch JM, Hubbard L, Nieto FJ. Retinal microvascular abnormalities and their relationship with hypertension, cardiovascular disease, and mortality. *Surv Ophthalmol*. 2001;46:59–80.
36. De Silva DA, Woon FP, Manzano JJ, et al. The relationship between aortic stiffness and changes in retinal microvessels among Asian ischemic stroke patients. *J Hum Hypertens*. 2012;26:716–722.
37. Cheung CY, Thomas GN, Tay W, et al. Retinal vascular fractal dimension and its relationship with cardiovascular and ocular risk factors. *Am J Ophthalmol*. 2012;154:663–674.
38. Crosby-Nwaobi R, Heng LZ, Sivaprasad S. Retinal vascular calibre, geometry and progression of diabetic retinopathy in type 2 diabetes mellitus. *Ophthalmologica*. 2012;228:84–92.
39. Leung H, Wang JJ, Rochtchina E, Wong TY, Klein R, Mitchell P. Impact of current and past blood pressure on retinal arteriolar

Investigative Ophthalmology & Visual Science

diameter in an older population. *J Hypertens*. 2004;22:1543–1549.

40. Schmidt D. The mystery of cotton-wool spots - a review of recent and historical descriptions. *Eur J Med Res*. 2008;13:231–266.
41. Tang J, Mohr S, Du YD, Kern TS. Non-uniform distribution of lesions and biochemical abnormalities within the retina of diabetic humans. *Curr Eye Res*. 2003;27:7–13.
42. Klein R, Meuer SM, Moss SE, Klein BEK. The relationship of retinal microaneurysm counts to the 4-year progression of diabetic retinopathy. *Arch Ophthalmol*. 1989;107:1780–1785.
43. Tarr JM, Kaul K, Wolanska K, Kohner EM, Chibber R. Retinopathy in diabetes. *Adv Exp Med Biol*. 2012;771:88–106.
44. Mendis KR, Balaratnasingam C, Yu P, et al. Correlation of histologic and clinical images to determine the diagnostic value of fluorescein angiography for studying retinal capillary detail. *Invest Ophthalmol Vis Sci*. 2010;51:5864–5869.
45. Chapman N, Dell'omo G, Sartini MS, et al. Peripheral vascular disease is associated with abnormal arteriolar diameter relationships at bifurcations in the human retina. *Clin Sci (Lond)*. 2002;103:111–116.
46. Grizzi F, Russo C, Colombo P, et al. Quantitative evaluation and modeling of two-dimensional neovascular network complexity: the surface fractal dimension. *BMC Cancer*. 2005;5:14.
47. Beard DA, Bassingthwaighte JB. Modeling advection and diffusion of oxygen in complex vascular networks. *Ann Biomed Eng*. 2001;29:298–310.
48. Levy MN, Sauceda G. Diffusion of oxygen from arterial to venous segments of renal capillaires. *Am J Physiol*. 1959;196:1336–1339.
49. Pannabecker TL, Dantzler WH. Three-dimensional architecture of collecting ducts, loops of Henle, and blood vessels in the renal papilla. *Am J Physiol Renal Physiol*. 2007;293:F696–F704.
50. Hudetz AG, Biswal BB, Feher G, Kampine JP. Effects of hypoxia and hypercapnia on capillary flow velocity in the rat cerebral cortex. *Microvasc Res*. 1997;54:35–42.
51. Atkinson JL, Anderson RE, Sundt TM Jr. The effect of carbon dioxide on the diameter of brain capillaries. *Brain Res*. 1990;517:333–340.
52. Stefanovic B, Hutchinson E, Yakovleva V, et al. Functional reactivity of cerebral capillaries. *J Cereb Blood Flow Metab*. 2008;28:961–972.
53. Duelli R, Kuschinsky W. Changes in brain capillary diameter during hypocapnia and hypercapnia. *J Cereb Blood Flow Metab*. 1993;13:1025–1028.
54. van der Linden P, De HS, Belisle S, et al. Comparative effects of red blood cell transfusion and increasing blood flow on tissue oxygenation in oxygen supply-dependent conditions. *Am J Respir Crit Care Med*. 2001;163:1605–1608.
55. Gariano RF, Gardner TW. Retinal angiogenesis in development and disease. *Nature*. 2005;438:960–966.
56. Mowat FM, Luhmann UF, Smith AJ, et al. HIF-1alpha and HIF-2alpha are differentially activated in distinct cell populations in retinal ischaemia. *PLoS One*. 2010;5:e11103.
57. le Noble F, Fleury V, Pries A, Corvol P, Eichmann A, Reneman RS. Control of arterial branching morphogenesis in embryogenesis: go with the flow. *Cardiovasc Res*. 2005;65:619–628.
58. Gerhardt H, Golding M, Fruttiger M, et al. VEGF guides angiogenic sprouting utilizing endothelial tip cell filopodia. *J Cell Biol*. 2003;161:1163–1177.
59. Kowalczuk L, Touchard E, Omri S, et al. Placental growth factor contributes to micro-vascular abnormalization and blood-retinal barrier breakdown in diabetic retinopathy. *PLoS One*. 2011;6:e17462.
60. Rousseau B, Larrieu-Lahargue F, Bikfalvi A, Javerzat S. Involvement of fibroblast growth factors in choroidal angiogenesis and retinal vascularization. *Exp Eye Res*. 2003;77:147–156.
61. Wang J, Xu X, Elliott MH, Zhu M, Le YZ. Muller cell-derived VEGF is essential for diabetes-induced retinal inflammation and vascular leakage. *Diabetes*. 2010;59:2297–2305.

Investigative Ophthalmology & Visual Science